Structural, elastic, piezoelectric and electronic properties of (B3) AlP compound under pressure

S. DAOUD*, N. BIOUD[a], N. LEBGAA[a]
Faculté des Sciences et de la Technologie, Université de Bordj Bou Arreridj, 34000, Algérie
[a]Laboratoire d'Optoélectronique & Composants, Université Ferhat Abbes- Sétif, 19000, Algérie

This paper carries out the First principles calculation of the crystal structure (zincblende (B3)) and phase transition of (B3) Aluminum phosphide based on the density functional theory (DFT) and density functional perturbation theory (DFPT). Using the relation between enthalpy and pressure, and the Born stability criteria, it finds that the transition phase from the B3 structural to the metallic nickel arsenic (NiAs) phase occurs respectively at the pressures of 6.62GPa and 22.25GPa. Then the elastic constants C_{11}, C_{12}, C_{44}, bulk modulus, shear modulus, anisotropy factor, piezoelectric coefficient and the linear and quadratic pressure coefficients of the energy bandgaps under pressures are discussed in detail. The results of the structural parameters, elastic and electronic properties are in good agreement with the available theoretical and experimental values. The maximum value of pressure is taken to be 9.50GPa, because beyond this value, the phase of AlP transforms from zincblende phase to nickel arsenic phase.

(Received November 12, 2013; accepted January 22, 2014)

Keywords: PP-PW method, Elastic and electronic properties, (B3) AlP compound

1. Introduction

Understanding the physical properties of semi-conductor compounds plays a vital role in developing new devices and technologies. Aluminum Phosphide is a wide-indirect band gap semiconductor $E_g^{ind} = 2.5eV$ [1, 2]. At normal conditions, AlP crystallizes in the zinc-blende structure [3, 4]. AlP is unstable in moist air, emitting poisonous phosphine gas, which has inhibited experimental studies of its high pressure structures [5]. The zincblende phase is known to transform to the nickel arsenic (NiAs) phase [6] (or from the zincblende phase to rocksalt phase [3]) at about 9.5±5 GPa [4]. The hexagonal nickel arsenide crystal structure ($P6_3mc$) can be thought of as an hcp stacking of anions with cations located in the octahedral interstices: each atom has six unlike nearest-neighbors while the cations have additional like-atom neighbors. It is unrelated to other structures observed in the III-V compounds, and has been reported in AlP, AlAs and AlSb. It represents an efficient packing of large anions and small cations, but the high pressure structures are generally metallic [5].

At a pressure of about 52GPa the NiAs phase has been reported to undergo a Cmcm-like distortion with no significant change in volume. The CsCl phase is a possible candidate for AlP at about 100GPa [5, 7].

Recently, Ameri et al [8] used a full-potential linear muffin-tin-orbital (FP-LMTO) method with both the local density approximation (LDA) and the generalized gradient approximation (GGA) to investigate the effect of increasing concentration of aluminum on the structural properties of $Al_xIn_{1-x}P$ Alloy. In the present work, we report first principles study of the hydrostatic pressure effect on the unit cell volume, crystal density, independent elastic constants, bulk modulus, shear modulus, anisotropy factor, piezoelectric coefficient, and the linear and quadratic pressure coefficients of the energy bandgaps and stability criteria for AlP compound in its structure zincblende phase, using the pseudopotential plane wave method, in the framework of the density functional theory within the local density approximation.

2. Computational methods

The first-principles calculations were performed by employing pseudopotential plane-waves approach based on the density functional theory (DFT) [9] and density functional perturbation theory (DFPT) [10] and implemented in the ABINIT code [11]. We used the Teter and Pade parameterization [12] for LDA. Only the outermost electrons of each atom were explicitly considered in the calculation. The effect of the inner electrons and the nucleus (the frozen core) was described within a pseudopotential scheme. We used the Trouiller Martins scheme [13] to generate the norm conserving nonlocal pseudopotentials. A plane-wave basis set was used to solve the Kohn-Sham equations in the pseudopotential implementation of the DFT-LDA.

The Brillouin zone integrations were replaced by discrete summations over a special set of k-points, using the standard k-point technique of Monkhorst and Pack [14] where the k-point mesh used is (6 × 6 × 6). The plane-wave energy cutoff to expand the wave functions is set to be 60 Hartree (1Hartree = 27.211396 eV, and $1eV = 1.602 \times 10^{-19}$ J). Careful convergence tests show that with these parameters relative energy converged to better than 10^{-5}eV/atom.

3. Results and discussions

3.1. Structural and electronic properties at *P=0*

After having determined the kinetic energy cut-off and the number of special k-points which gives the best convergence possible of total energy, they are used to calculate the total energy for various values of the lattice constant. Energies were calculated for various values of the lattice constant, the different values obtained are then traced as a function of the unit cell volume. One can deduce the static structural properties such as the equilibrium lattice constant from the volume which gives the minimum energy, the bulk modulus B_0 and its pressure derivatives $B_0^{'}$. With the fitting on the values of total energy as a function of the unit cell volume using the following Murnaghan equation [15]

$$E(V) - E(V_0) = \frac{B_0 V}{B_0^{'}}\left[\frac{(V_0/V)^{B_0^{'}}}{B_0^{'}-1}+1\right] - \frac{B_0 V_0}{B_0^{'}-1} \qquad (1)$$

$$B_0 = V\frac{\partial^2 E}{\partial V^2} = \frac{4}{9a}\frac{\partial^2 E}{\partial a^2} \qquad (2)$$

Where B_0 is the bulk modulus given by the relation (2) at *P=0*, V_0 is the equilibrium volume, $E(V_0)$ is the energy in equilibrium volume, $B_0^{'}$ is the pressure derivatives of the bulk modulus at *P=0* and, *a* is the lattice constant. The figure1 watches the evolution of the total energy as a function of the unit cell volume of the (B3) AlP.

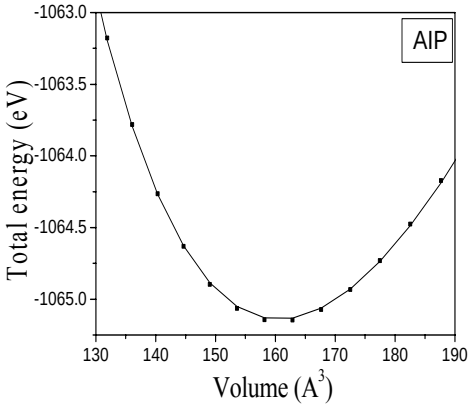

Fig. 1. Total energy varying with the unit cell volume of the (B3) AlP compound.

The results for: lattice parameter a_0, bulk modulus B_0, and its pressure derivative B_0' are reported in table.1 and compared with the available experimental [16, 17] and theoretical data [3, 6-8, 18-32].

As can be seen, our calculated equilibrium lattice parameter a_0 (10.27255Bohr = 5.436Å) is in good agreement with the previous calculations data: the value obtained in this work of lattice constant is equal exactly the value of the Ref [22] and it deviates from the calculated [30] and [27] ones within 0.11% and 0.30% respectively. As can be seen, also that our calculated bulk modulus B_0 obtained from the equation (2) and from the equation (8) are also in good agreement with the previous calculations, they are deviate from the calculated [27] within 0.24% and 3.74% respectively. The pressure derivatives of the bulk modulus B_0' is also in good agreement with the available theoretical data [6, 22]. The above results also show that the computational methods and parameters used in this paper are reasonable.

The electronic and optical properties of the semiconductors have been the subject of great interest, both experimental and theoretical, because of their technological importance [33]. The result for: the energy band gaps obtained in this work is reported also in table.1 and compared with the available experiments [1, 2, 16], and theoretical data [3, 8, 22, 28-30]. At the equilibrium volume, the minimum of the conduction band is found to be at the X point, rendering this compound an indirect semiconductor with a ($\Gamma_v \rightarrow X_c$) optical transition of 1.408eV, this value is in good agreement with the previous calculations (1.41eV) of the reference [30], and the deviation is only 0.14%.

*Table 1. Lattice constants a_0, bulk modulus B_0 and its pressure derivative B_0', and the energy band gaps E_g of (B3) AlP at P=0 in comparison with the available, experiments [1, 2, 16, 17] theoretical values [3, 6-8, 18-32] [a] from the equation (2), [b] from the equation (8), * at room temperature.*

Parameter				
a_0 (Å)	5.436	5.453[3]	5.471[6]	5.45[7]
	5.449[8]LDA	5.534[8]GGA	5.467 [16]	
	5.4625[17]*	5.4635[18]	5.451[19, 20]	
	5.436[22]	5.462[23]	5.44285[24]	
	5.417[25]	5.508[26]	5.42[27]	
	5.520[28]	5.4131[29]	5.43[30]	
	5.40[31]	5.48[32]		
B_0 (GPa)	86.29 [a]	89.74[b]	87.8[3]	
	86.5[6]	90[7]	87.067[8]LDA	
	81.89[8]GGA	86[20]	89[22]	
	95.46[24]	88.6[25]	81.52[26]	
	90.46[30]	90[31]	88[32]	
B_0'	4.05	3.852[3]	4.18 [6]	4.34[21]
	4.14[22]	3.72[30]		
E_g	1.408	2.50[1]	.500[2]	6.6075[3]
	1.4658[8]LDA	1.6386[8]GGA	2.52[16]	
	2.43[17]*	1.44[22]	1.4194[29]	1.41[30]

It is clearly seen that the band gaps are on the whole underestimated in comparison with experiments results [1, 2, 16, 18]. This underestimation of the band gaps is mainly due to the fact that both the simple form of LDA or GGA do note take into account the quasi-particle self energy correctly [34] which make them not sufficiently flexible to accurately reproduce both exchange and correlation energy and its charge derivative. The calculated energy band gaps for AlP compound is in general in good agreement with the available theoretical results [3, 8, 22, 28-30].

To illustrate the degree of covalency in this compound, Fig. 2 shows the typical features of the ionicity bonded semiconductors. The net charge transfer from the cation (Aluminum, Al) to the anion (Phosphorus, P), which indicates the degree of the ionicity of the bonding, it is relatively as large as suggested by Fig. 2; there remains a considerable (*fi* = 0.421[35], or *fi* is the Phillips ionicity) degree of ionic character in the cation-anion bond, and we notice that the chemical bonding is strongly ionic, i.e. a much charge is transferred from the Aluminum to Phosphorus.

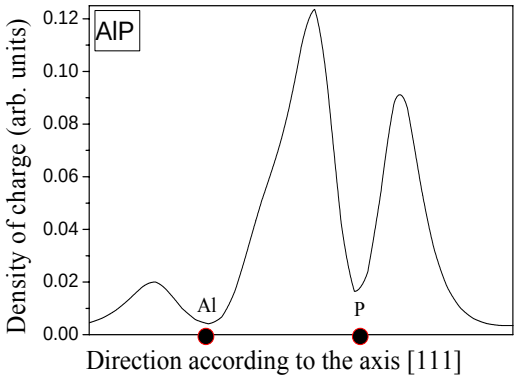

Fig. 2. Total valence charge densities along the <111> direction at equilibrium volume

3.2. Hydrostatic pressure effect

3.2.1 Pressure of the phase transition

The stability of an particular structure is decided by the minimum of the Gibbs energy, which is given as [5]

$$G = U + PV - TS \tag{3}$$

Where : U is the total internal energy, P the pressure, T the temperature, S the entropy, and V the volume.

When structures are considered by calculation at 0K, it is possible that they are unstable with respect to symmetry-breaking strain (elastic instability), atomic motion (phonon instability) or some combination. It is also possible that such instabilities develop with increasing pressure [5].

To investigate the pressure-induced structural transition, we optimized both the cell parameters and atomic positions for ZB and the metallic nickel arsenic (NiAs) phases under each hydrostatic pressure. The computed relative enthalpy versus pressure curves for both phases is shown in Fig. 3. The transition pressure is a pressure at which curves for both phases crosses. As is shown in Fig. 4, the phase-transition pressure from ZB to the metallic nickel arsenic (NiAs) structure is found to be 6.62GPa.

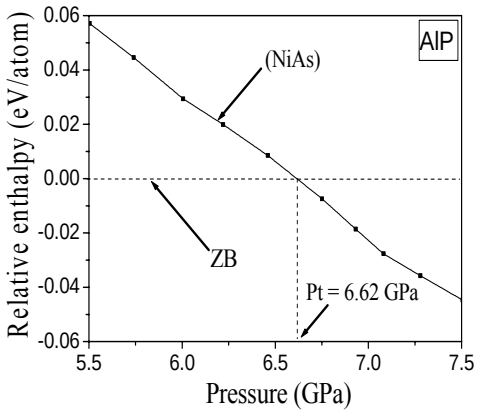

Fig. 3. Relative enthalpy of metallic nickel arsenic (NiAs) phase with respect to ZB structure. The crossing of ZB and nickel arsenic (NiAs) phases occurs at about 6.62GPa.

3.2.2 Structural properties

In order to further validate the reliability and accuracy of our calculated structural properties, the calculated unit cell volumes under a series of applied hydrostatic pressures were used to construct the P-V data set, which was subsequently fitted by the Murnaghan equation [36]

$$P(V) = \tfrac{3}{2}B_0\left[\left(\left(\frac{V_0}{V}\right)^{\frac{7}{3}} - \left(\frac{V_0}{V}\right)^{\frac{5}{3}}\right)\right]\left\{1 + \tfrac{3}{4}(B_0^{'} - 4)\left[\left(\left(\frac{V_0}{V}\right)^{\frac{2}{3}} - 1\right)\right]\right\} \tag{4}$$

Where: B_0 is the bulk modulus at $P = 0$, $B_0^{'}$ is its pressure derivative at $P = 0$, V_0 is the volume of unit cell, is fixed at the value determined from the $P = 0$ data, and V is the volume of unit cell at $P \neq 0$.

In order to show how the structural parameter in this com-pound behave under pressure, the equilibrium geometries of (B3) AlP unit cells were computed at fixed values of applied hydrostatic pressure in the 0 to 9.50GPa range, where, at each pressure, a complete optimization for the volume unit cells was performed. In Fig. 4, we plot the variation of the unit cell volume and the relative unit cell volume versus the applied hydrostatic pressure.

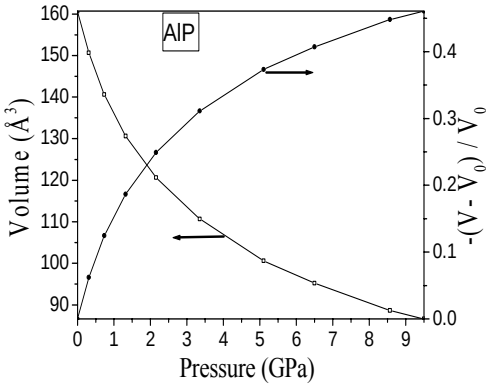

Fig. 4. Pressure-volume dependence and the relative unit cell volume versus applied hydrostatic pressure.

The structure and composition of crystals can be used to calculate the density g, which is the mass divided by the volume, it is given as [37]

$$g = \frac{Z.M.u}{a.b.c.\sqrt{\sin^2\alpha + \sin^2\beta + \sin^2\gamma - 2(1 - \cos\alpha.\cos\beta.\cos\gamma)}} \quad (5)$$

where Z is the number of formula units in a crystal unit cell, M is the molecular weight of a formula unit in amu, u is weight of an amu, a , b , and c are unit cell axes lengths, and α, β and γ are unit cell axes angles.

In general, the pure amorphous materials have lower density than the corresponding crystalline materials.

The X-ray crystal density g can be simply written, in terms of d_M, as [38]

$$g = Md_M / N_A = 4M / N_A V \quad (6)$$

Where M is the molecular weight (for AlP, M= 57.9552 uma), N_A=6.022×10^{23}mol^{-1} is the Avogadro constant, V is the unit cell volume, and d_M is the molecular density. For the zincblende-type semiconductors (d_M = 4/a^3, where a is the lattice parameter).

The calculated crystal density at different values of pressure, for (B3) AlP is plotted in Fig. 5.

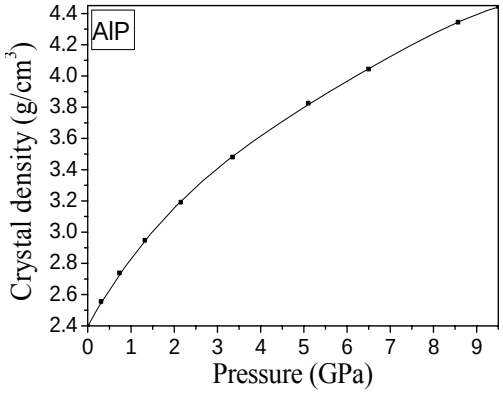

Fig. 5. Crystal density varying with the hydrostatic pressure of the (B3) AlP compound.

For AlP, at $P = 0$, g = 2.397g/cm^3, this value is in good agreement with the previous calculations data, it deviates from the results 2.3604 g/cm^3 and 2.40g/cm^3 of the Refs [39] and [40] ones within 1.53% and 0.14% respectively.

3.2.3 Elastic properties

There are different methods to obtain the elastic constant through the first principle. Nielsen and Martin [41] developed a method using strain-stress relation.

Recently, Hamman et al. [42] developed a reduced coordinate metric tensor method for the linear response formulation of strain type perturbations which could be calculated by the DFPT method. The elastic constants reported in this article are obtained by the method used by the Ref [43] as implemented in the ABINIT code. The elastic stiffness tensor of a cubic structure has three independent components, namely C_{11}, C_{12} and C_{44} in Young's notation. The obtained elastic constants C_{ij}, of (B3) AlP at different pressure are presented in figure 6. As shown in this figure, we find, that all the elastic constants C_{ij} increase gradually with the increasing of the pressure up to 9.50GPa.

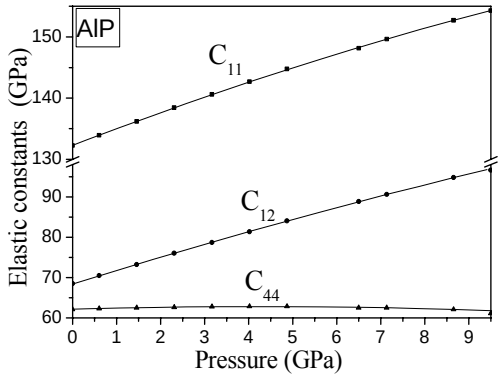

Fig. 6. Elastic constants C_{ij} versus the pressure of (B3) AlP

The shear modulus is also known as the rigidity. For cubic single crystal, the shear modulus G and the elastic constants C_{11}, and C_{12} are related by the following relation [38]

$$G = (C_{11} - C_{12}) / 2 \quad (7)$$

The obtained values of the shear modulus G of (B3) AlP at different pressure are presented in figure 7.

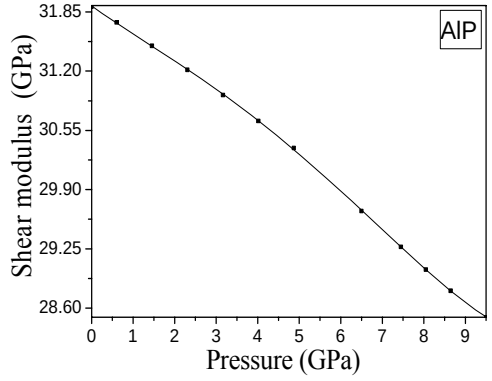

Fig. 7. Shear modulus G versus the hydrostatic pressure of the (B3) AlP compound.

Bulk modulus describes the elastic properties of a solid when it is under pressure. For cubic crystals the bulk modulus B, and the elastic constants are related by [38]

$$B = [(C_{11} + 2C_{12}) / 3] \quad (8)$$

The obtained values of bulk modulus B of (B3) AlP at different pressure are presented in Fig. 8.

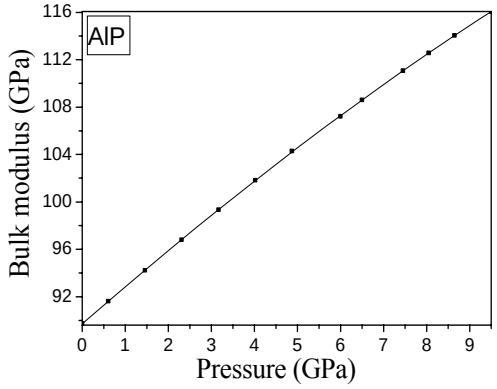

Fig. 8. Bulk modulus B versus the pressure of (B3) AlP

The Zener anisotropy factor (Z), which is the square of the ratio of the acoustic velocity of the transverse mode propagating along [100] and that of the transverse mode propagating along [110] with $[1\,\bar{1}\,1]$ polarization [44]. Through the elastic constants, we can obtain the zener anisotropy parameter.

For cubic single crystal, this parameter can be calculated by using the following equation: [45]

$$Z = 2C_{44}/(C_{11} - C_{12}) \tag{9}$$

The obtained values of the Zener anisotropy factor at different values of pressure are presented in fig. 9.

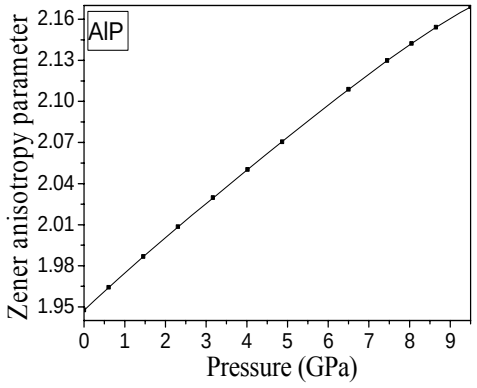

Fig. 9. Zener anisotropy parameter versus the hydrostatic pressure of the (B3) AlP

If $Z < 1$ the crystal is stiffest along <100> cube axes, and when $Z > 1$, it is stiffest along the <111> body diagonals. The body-centered cubic alkali metals (Li, Na, K) are much stiffer along <111> directions, as are the column IV elements (C, Si, Ge) with the diamond structure [45]. In both structures the nearest-neighbor bonds are also in <111> directions. For alkali halide crystals with the rocksalt structure (NaCl, KCl, RbCl), the cation-anion bonds are oriented along <100> directions [45].

The values of the Z varies from 1.95 ($Z > 1$) at zero pressure, which corresponds to an almost anisotropic solid, to 2.17 at 9.50GPa, which induced a small increasing of the ratio between the longitudinal acoustic velocities along [110] and [100] in this compound.

The usual Born description for the stability of a cubic crystal is expressed in terms of elastic constants as follows [3]

$$B_T = (C_{11} + 2C_{12})/3 > 0,\ G = (C_{11} - C_{12})/2 > 0,\quad C_{44} > 0 \tag{10}$$

where C_{ij} are the conventional elastic constants and B_T is the bulk modulus. The quantities C_{44} and G are the shear and tetragonal moduli of a cubic crystal. These conditions are known as the spinodal, shear and Born criteria respectively. Wang et al [46], showed that under external pressure these relations need to be modified to describe changes in enthalpy rather than energy.

When deformation is expressed, the new stability criteria for crystals under hydrostatic pressure have considered. To study the stability of (B3) AlP compound, the calculated values of the elastic constants at normal and under hydro-static pressure were compared with the generalized elastic stability criteria using the following relations [47]:

$$K = (C_{11} + 2C_{12} + P)/3 > 0,\quad G = (C_{11} - C_{12} - 2P)/2 > 0,$$
$$G' = C_{44} - P > 0 \tag{11}$$

The obtained values of the generalized elastic stability criteria of Born at different values of pressure are presented in Fig. 10.

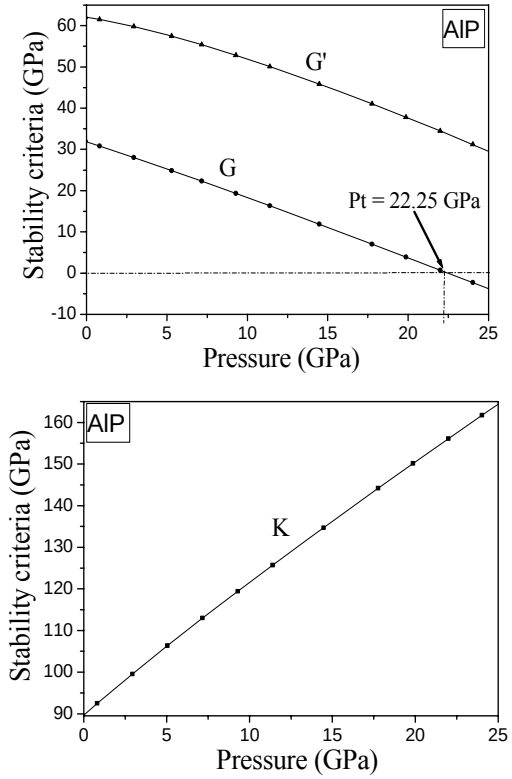

Fig. 10. Born stability criteria, G, G′ and K varying with the pressure of the (B3) AlP compound.

The requirement of mechanical stability in a cubic crystal leads to the following restrictions on the elastic constants, C_{11}-$C_{12} > 0$, $C_{11} > 0$, $C_{44} > 0$, $C_{11} + 2C_{12} > 0$ [48]. The elastic constants at zero-pressure obey these stability conditions, including the fact that C_{12} must be smaller than C_{11}. Our calculated elastic constants also obey the cubic stability conditions, meaning that $C_{12} < B < C_{11}$. As pressure is applied to (B3) AlP compound, it transforms from (B3) phase to the metallic nickel arsenic (NiAs) phase [6].

As shown in Fig. 10, we find that G decreases gradually with the pressure and vanishes at about 22.25GPa, and G´ also decreases to zero but at a higher pressure. Therefore, the phase transition occurs at a much higher pressure of 22.25 GPa. This value obtained of the transition pressure P_t (GPa) is listed and compared with others experimental [4, 5, 53, 54] theoretical [6, 7, 30, 49-52] data in Table 2.

Table 2. Transition pressure P_t (GPa) of (B3) AlP in compa-rison with experimental [4, 5, 53, 54], and theoretical [6, 7, 30, 49-52] data. [a] from the Relative enthalpy method, [b] from generalized elastic stability of Born. [c] from the equation (12)

Our work	6.62[a]	22.25[b]	19.04[c]
Other works	9.5±5[4]exp	14[5, 53]exp	9.3 [6]
	7.7[7] 8.3[49]	(9.5 - 17)[50]	6.78 [30]
	< 43[51]	18.1 [52]	17.0±0.5 [54]exp

For some group-IV, A^{II} B^{VI} and A^{III} B^{V} semiconductors, the transition pressure to the first phase observed versus the bulk modulus B (B in GPa), it can be deduced from the following empirical relation [55]

$$P_t = 0.1\left(B/(99 - (\lambda + 79))\right)^3 \qquad (12)$$

where P_t is the transition pressure in GPa, and λ is a parameter appropriate ($\lambda = 5$) for the A^{III}-B^{V} semiconductors.

Using this formula, with the bulk modulus calculated from the relation of equation (2), the obtained value of the transition pressure P_t of (B3) AlP is listed and compared with other values of the literature.

From the generalized elastic stability of Born, there is a metallization phase transition at around 22.25GPa; the most likely candidate is the NiAs structure. It is clearly seen that our result (22.25GPa) is substantially very higher than the value of 6.62GPa obtained from the relative enthalpy method, but the later (6.62GPa) is in agreement comparatively with the theoretical results of the Refs [7, 30, 49]; but, it is very lower than the experimental values [14, 54].

It is clearly seen also, that our result (19.04GPa) calculated from the relation of equation (12), is also very higher than the value of 6.62GPa predicted on the basis of thermodynamic criteria, but it is in good agreement comparatively with the results obtained from the generalized elastic stability of Born. This value is also in good agreement with the value (18.1GPa) of the reference [52], and the deviation is only 5.19%.

3.2.4 Piezoelectric coefficient

Among the five symmetry classes belonging to the cubic system, only $\bar{4}$ 3m and 23 classes exhibit the piezoelectric effect, for the others (i.e., m3m, 432, m3) the piezoelectric effect being absent. In the first case, the piezoelectric tensor contains only one constant e_{14}, is expressed C/m^2, which is given as [56]

$$e = \begin{pmatrix} 0 & 0 & 0 & e_{14} & 0 & 0 \\ 0 & 0 & 0 & 0 & e_{14} & 0 \\ 0 & 0 & 0 & 0 & 0 & e_{14} \end{pmatrix} \qquad (13)$$

The effect of the pressure on the piezoelectric coefficient e_{14} for AlP is presented in Fig. 11.

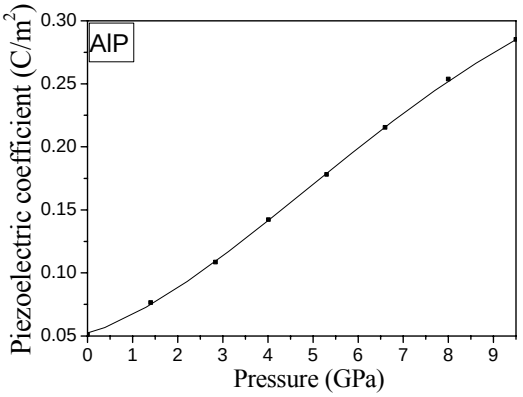

Fig. 11. Effect of the hydrostatic pressure on the piezoelectric coefficient e_{14} for (B3) AlP.

3.2.5 Electronic properties

In order to investigate the effects of the hydrostatic pressure on the size of the energy gap and position of the conduction band minimum of the AlP compound, the band energies at selected symmetry points are examined as a function of the pressure. The results of our calculation for the direct and indirect bandgaps along the high symmetry directions in the Brillouin zone for AlP versus the hydrostatic pressure up to 9.50GPa are shown in Fig. 12.

As for typical semiconductors, the fundamental gap decreases when the pressure increase (volume is compressed). The behavior of the bandgap variation under high hydro-static pressure is very similar to that found in other III-V materials [47].

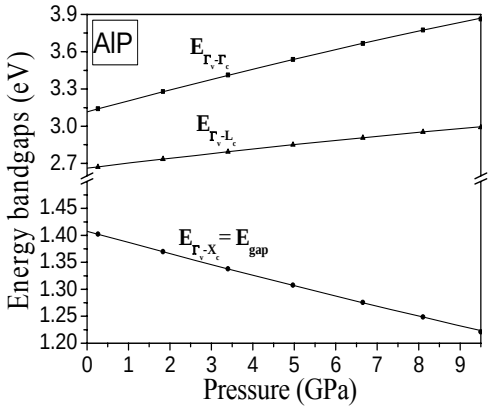

Fig. 12. Pressure dependence of the Energy bandgaps $E_{\Gamma-\Gamma}$, $E_{\Gamma-L}$ and optical energy bandgap $E_g = E_{\Gamma-X}$

For most semiconductors, the variation of the different band gaps under pressure can be described by the following quadratic expression [47, 57]:

$$E_i(P) = E_i(0) + c_1 P + c_2 P^2 \quad (14)$$

Where: c_1 and c_2 are respectively the linear and quadratic pressure coefficients, they are given by:

$$c_1 = \partial E_i/\partial p, \quad c_2 = \partial^2 E_i/\partial p^2 \quad (15)$$

The results for: the linear and quadratic pressure coefficients are reported in Table 3.

Table 3. Linear and quadratic pressure coefficients of different bandgaps of (B3) AlP compound.

	$\Gamma_V \rightarrow \Gamma_C$	$Eg=\Gamma_V \rightarrow X_C$	$\Gamma_V \rightarrow L_C$
E(0)	3.115	1.408	2.663
c_1 (eV.Mbar^{-1})	0.091	-0.021	0.0406
c_2 (eV.Mbar^{-2})	-0.001	0.0002	-0.0006

4. Conclusions

A summary of obtained results in this work is given here in as follows:

The calculated equilibrium lattice constant, the bulk modulus and its pressure derivatives at $P = 0$ are in good agreement with the previous calculations reported in the literature.

The pressures phase transition from the zincblende phase (B3) to the nickel arsenic (NiAs) phase of this compound are obtained from three methods, they are respectively at around 6.62GPa, 22.25GPa and 19.04 GPa. The first value is generally in good agreement with the available theoretical data reported in the literature, but the second, and the third values are very higher than the available experimental and theoretical data reported in the literature.

The calculated unit cell volumes under a series of applied hydrostatic pressures were used to construct the P-V data set, which was fitted by the Murnaghan equation.

The crystal density, the independent elastic stiffness constants, the bulk modulus, the zener anisotropy factor, and the piezoelectric coefficient increase with the increasing of the hydrostatic pressure.

The energy bandgap at the equilibrium volume is obtained, the minimum of the conduction band is found to be at X point, rendering this compound an indirect semiconductor with an indirect ($\Gamma_v \rightarrow X_c$) optical transition of 1.408eV, this value is also in good agreement with the previous calculations, but it is under-estimate in comparison with the experiment results.

The effects of the hydrostatic pressure on the size of the energy gap and position of the conduction band minimum of the (B3) AlP compound are investigated. The linear and quadratic pressure coefficients are also determined, the results obtained are generally in good agreement with available theoretical data reported in the literature.

Acknowledgements

The authors are thankful to Université Catholique de Louvain, Corning Incorporated, and other contributors for the ABINIT computer code.

References

[1] R. W. G. Wyckoff, Crystal Structures, Second Edition Krieger, Malabar, 1986.
[2] S. N. Rashkeev, W. R. L. Lambrecht, Phys. Rev. B, **63** (16), 165212 (2001).
[3] H. R. Jappor, M. A. Abdulsattar, A. M. Abdullettif, Open Condens Matter Phys J, **3,** 1 (2010).
[4] R. G. Greene, H. Luo, A. L. Ruoff, J. Appl. Phys, **76**, 7296 (1994).
[5] G. J. Ackland, Reports on Progress in Physics, **64**, 483 (2001**)**; G. J. Ackland, High Pressure Phases of Group IV and III-V Semiconductors (UK: The University of Edinburgh, Scotland) REVTEX 3.0 1, 1992.
[6] S. B. Zhang, M. L. Cohen, Phys. Rev. B **35**(14), 7604 (1987).
[7] A. Mujica, P. Rodríguez-Hernández, S. Radescu, R. J. Needs, A. Muñoz, Phys Stat Solidi (b), **211**, 39 (1999).
[8] M. Ameri, A. Bentouaf, M. Doui-Aici et al., Mater. Sci & Application, **2**, 729 (2011).
[9] E. Engel, R. M. Dreizler, Density Functional Theory, New York: Springer-Verlag Berlin Heidelberg, 2011.
[10] S. Baroni, P. Giannozzi, A. Testa, Phys. Rev. Lett, **58**(18), 1861 (1987).
[11] X Gonze et al., Comput. Mater. Sci, **25**, 478 (2002).
[12] J. P. Perdew, K. Burke, M. Ernzerhof, Phys. Rev. Lett, **77**, 3865 (1996).
[13] N. Troullier, J. L. Martins, Phys. Rev. B **43**, 1993 (1991).

[14] H. J. Monkhorst, J. D. Pack, Phys. Rev. B **13**, 5189 (1976).
[15] F. Murnaghan, Proc. Nat. Acad. Sci, **30**, 244 (1944).
[16] I. Vurgaftman, J. R. Meyer, L. R. Ram-Mohan, Jour. of Appl. Phys, **89** (11), 5815 (2001).
[17] A. R. Degheidy, A. M. Elabsy, H. G. Abdelwahed E. B. Elkenany, Indian J. Phys, **86** (5), 363 (2012).
[18] V. N. Bessolov, S. G. Konnikov, V. I. Umpanki Yu P. Yakovlev, Sov. Phys. Solid State, **24**, 875 (1982).
[19] S. M. Sze, Physics of Semiconductor Device, Wiley Interscience Publication, New York, 1981.
[20] S. Froyen, M. Cohen, Phys. Rev. B, **28**, 3258 (1983)
[21] M. Causa, A. Zupan, Chem. Phys. Lett, **220**, 145 (1994).
[22] R. Ahmed, F. Aleem, S. Hashemifar, H. Akbarzadeh, Physica B, **403**, 1876 (2008).
[23] M -Z. Huang, W. Y. Ching, Phys. Rev. B, **47**(15), 9449 (1993).
[24] V. Khanin, S. E. Kulkova, Russ Phys J, **48**(1), 61 (2005).
[25] S. O. Wang, H. O. Ye, Phys. Rev. B, **66** (23), 235111 (2002).
[26] L. H. Yu, K. L. Yao, Z. L. Liu, Solid State Comm, **135** (1-2), 124 (2005).
[27] S. Froyen, M. L. Cohen, Phys. Rev B, **28** (6), 3258 (1983).
[28] O. Madelung, L. Bornstein, Semiconductors, Physics of Group IV Elements and III-V Compounds, Vol. **17**, New Series, Group III, Springer Verlag, Berlin 1982.
[29] S. Z. Karazhanov, L. C. Lew Yan Voon, Semiconductors, **39**(2), 161 (2005).
[30] S. Aouadi, P. Rodriguez-Hernandez, K. Kassali, A. Muñoz, Physics Letters A, **372**(32), 5340 (2008).
[31] P. Rodriguez-Hernández, A. Muñoz, Semic. Scie. And Techn, **7** (12), 1437 (1992).
[32] L. Börstein, Semicondutors Physics of Group IV Elements and III-V Compounds, Vol. III/17a, Springer-Verlag, Berlin, 1992.
[33] W. A. Harrison, Electronic Structure and the Properties of Solids, Freeman, San Francisco, 1980.
[34] M. Grundmann, The Physics of Semiconductors, Springer-Verlag, Berlin Heidelberg, 2006.
[35] N. E. Christensen, S. Satpathy, Z. Pawlowska, Phys. Rev. B, **36** (2), 1032 (1987).
[36] F. Birch, J. J. Geophys. Res, **83**, 1257 (1978).
[37] W. J. Tropf, M. F. Thomas, T. J. Harris, Properties Of crystals and glasses, Handbook of Optics, Vol. IV, Mc Graw-Hill, New York, 2004.
[38] S. Adachi, Physical properties of III-V semiconductor Compounds, New York: John Wiley & Sons, 1992.
[39] S. Adachi, Properties of Semiconductor Alloys: Group IV, III–V and II–VI Semiconductors, John Wiley & Sons, 2009.
[40] R. J. Caveney, Philos. Mag, **17**, 943 (1968).
[41] O. H. Nielsen and R. M. Martin, Phy. Rev. B, **32**, 3792 (1985).
[42] D. R. Hamman, X. Wu, K. M. Rabe, D. Vanderbilt, Phys. Rev. B, **71**, 035117 (2005).
[43] A. Benamrani, K. Kassali, Kh. Bouamama, High Pressure Res, **30** (1), 207 (2010),
[44] S. Speziale, S. R. Shieh and T. S. Duffy, J. of Geo. Res, **111**, 1 (2006).
[45] R. E. Newnham, Properties of materials: Anisotropy, Symmetry, Structure, Oxford University Press, 2005.
[46] J. Wang, S. Yip, S. R. Phillpot, D. Wolf, Phys. Rev. Lett, **71**, 4182 (1993).
[47] S. Daoud, K. Loucif, N. Bioud, N. Lebgaa, L. Belagraa, Pramana J. Phys, **79** (1), 95 (2012).
[48] M. Born and K. Huang, Dynamical Theory of Crystal Lattices, Clarendon: Oxford, 1954.
[49] P. E. Vancamp, V. E. Vandoren, Solid State Comm, **95** (3), 173 (1995).
[50] M. Baublitz and A. Ruoff, J. Appl. Phys, **53**, 6179 (1982).
[51] A. Mujica, Angel Rubio, A. Muñoz. R. J. Needs Rev. Mod. Phys, **75** (3), 863 (2003).
[52] A. Zunger, K. Kim, V. Ozolins, Phys Status Solidi (b), **223**, 369 (2001).
[53] J. Wanagel, V. Arnold, A. L. Ruoff, J. Appl. Phys, **47**, 2821 (1976).
[54] S. C. Yu, I. L. Spain, E. F. Skelton, Sol. Stat. Commun, **25**, 49 (1978).
[55] A. S. Verma, B. K. Sarkar, V. K. Jindal, Physica B, **405**, 1737 (2010).
[56] J. Yang**,** Special Topics in the Theory of Piezoelectricity, Springer Science + Business Media, LLC, p194, 2009.
[57] S. Labidi, H. Meradji, S. Ghemid, S. Meçabih, B. Abbar J. Optoelectron. Adv. Mater. **11**, 994 (2009).

*Corresponding author: salah_daoud07@yahoo.fr